

5-1-2000

# Charge-Transfer Bonding in Metal–Arene Coordination

S. M. Hubig  
*University of Houston*

Sergey V. Lindeman  
*Marquette University, sergey.lindeman@marquette.edu*

Jay K. Kochi  
*University of Houston*

---

Accepted version. *Coordination Chemistry Reviews*, Vol. 200-202 (May 2000): 831-873. DOI. © 2018 Elsevier B.V. Used with permission.

Sergey V. Lindeman was affiliated with the University of Houston at the time of publication.

Marquette University

**e-Publications@Marquette**

***Chemistry Faculty Research and Publications/College of Arts and Sciences***

***This paper is NOT THE PUBLISHED VERSION; but the author's final, peer-reviewed manuscript.*** The published version may be accessed by following the link in the citation below.

*Journal of the American Chemical Society*, Vol. 125, No. 38 (2003): 11597-11606. [DOI](#). This article is © American Chemical Society and permission has been granted for this version to appear in [e-Publications@Marquette](#). American Chemical Society does not grant permission for this article to be further copied/distributed or hosted elsewhere without the express permission from American Chemical Society.

# The Charge-Transfer Motif in Crystal Engineering. Self-Assembly of Acentric (Diamondoid) Networks from Halide Salts and Carbon Tetrabromide as Electron-Donor/Acceptor Synthons

**Sergey V. Lindeman**

Department of Chemistry, University of Houston, Houston, Texas

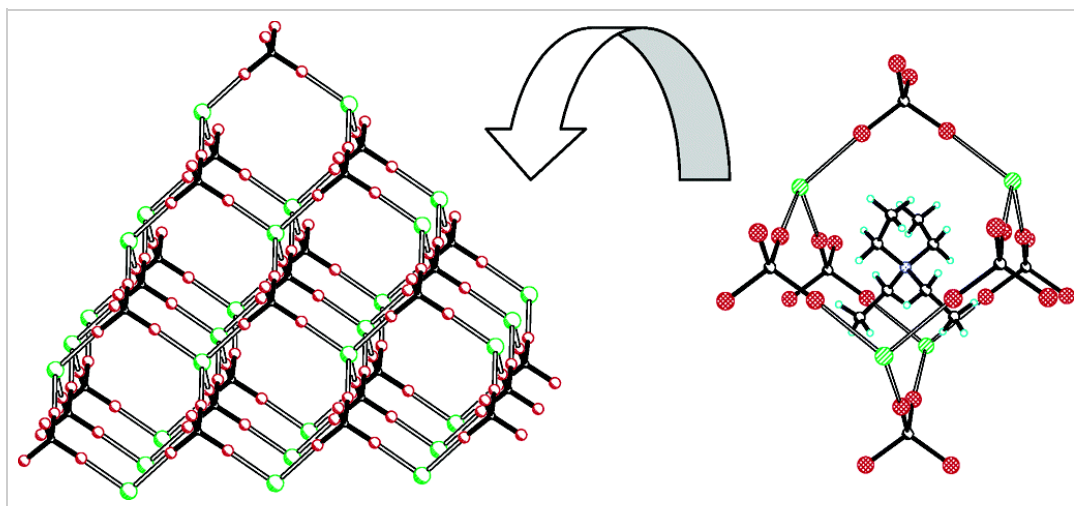
**Jürgen Hecht**

Department of Chemistry, University of Houston, Houston, Texas

**Jay K. Kochi**

Department of Chemistry, University of Houston, Houston, Texas

## Abstract



Unusual strength and directionality for the charge-transfer motif (established in solution) are shown to carry over into the solid state by the facile synthesis of a series of robust crystals of the [1:1] donor/acceptor complexes of carbon tetrabromide with the electron-rich halide anions (chloride, bromide, and iodide). X-ray crystallographic analyses identify the consistent formation of diamondoid networks, the dimensionality of which is dictated by the size of the tetraalkylammonium counterion. For the tetraethylammonium bromide/carbon tetrabromide dyad, the three-dimensional (diamondoid) network consists of donor (bromide) and acceptor ( $\text{CBr}_4$ ) nodes alternately populated to result in the effective annihilation of centers of symmetry in agreement with the sphaleroid structural subclass. Such inherently acentric networks exhibit intensive nonlinear optical properties in which the second harmonics generation in the extended charge-transfer system is augmented by the effective electronic (HOMO–LUMO) coupling between contiguous  $\text{CBr}_4$ /halide centers.

## Introduction

Tetrahedrally shaped molecular and ionic entities can be self-assembled to form highly symmetrical crystalline networks in the same fashion that  $\text{sp}^3$ -hybridized carbon atoms are covalently linked in the diamond (crystal) structure. Thus, Ermer<sup>1</sup> first showed how tetracarboxylic acids derived from adamantane and neopentane form diamondoid networks interconnected by (strong) double hydrogen bonds between the terminal carboxy groups (see Chart 1). This approach has also been used by Wuest,<sup>2</sup> Desiraju,<sup>3</sup> Galoppini,<sup>4</sup> and co-workers, who employed substituted tetraphenylmethanes as building blocks coupled with an array of attractive intermolecular forces. The second approach exploits intermolecular interactions, not directly between the tetrahedral building blocks, but through appropriate (linear) spacers. In this way, Kitazawa, Iwamoto, et al.<sup>5</sup> utilized coordination compounds in which identical tetrahedral metal centers ( $\text{Cd}^{2+}$ ) are linked through linear bidentate ligands (CN<sup>-</sup>). Variation of the symmetry of the bridging ligands/molecules then results in two different structural classes – cubic silica-related structures from symmetric bridges and cubic ice-related structures from asymmetric bridges (see Chart 2). The concept of symmetric bridging was developed by Zaworotko and co-workers<sup>6</sup> for tetrahedral Mn-clusters hydrogen-bonded through a variety of organic spacers, by Ciani et al.<sup>7</sup> for some silver(I) complexes, and by Aoyama et al.<sup>8</sup> for purely organic systems. The use of asymmetric bridging by Evans, Lin, et al.<sup>9</sup> exploits the intrinsic lack of inversion symmetry to

produce an interesting array of noncentrosymmetric Cd and Zn complexes for nonlinear optical applications. Recently, Desiraju, Clearfield, and co-workers<sup>10</sup> also attempted the ice-related assembly of asymmetric tetraphenylmethane moieties. The third (and the least developed) approach was formulated by Hoskins and Robson<sup>11</sup> who interconnect tetrahedral organic (tetraarylmethane) or coordination (zinc cyanide) blocks, not through linear, but through tetrahedral copper(I) "joints" that result in diamondoid networks with alternate tetrahedral nodes (see Chart 3).<sup>13</sup> These distinctive arrays in fact belong to the sphalerite (ZnS)<sup>12</sup> structural subclass of diamondoid networks which intrinsically lack inversion centers. [Yet this important point seems to have been overlooked by recent investigators.<sup>14</sup>]

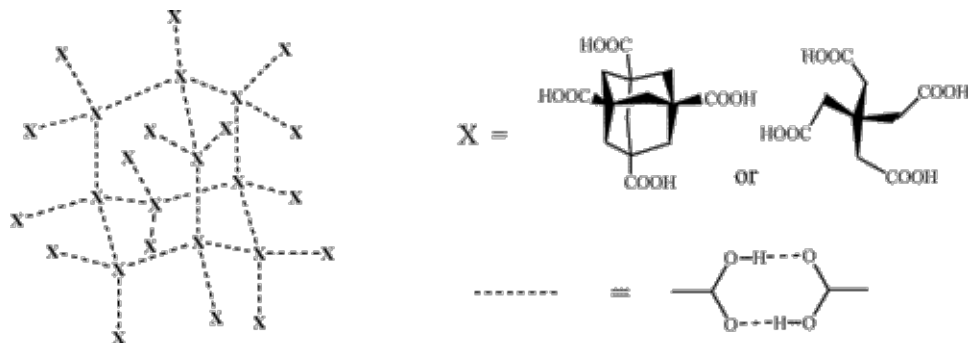


Chart 1

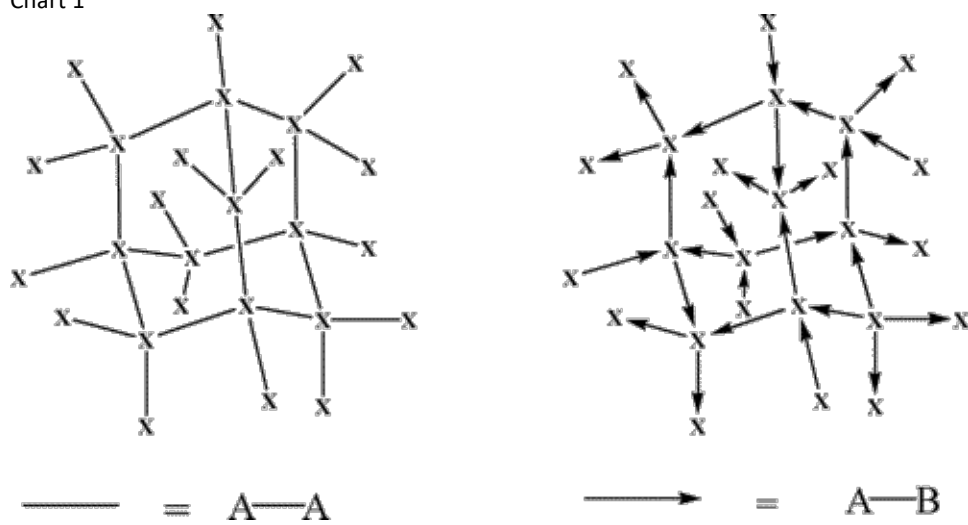


Chart 2

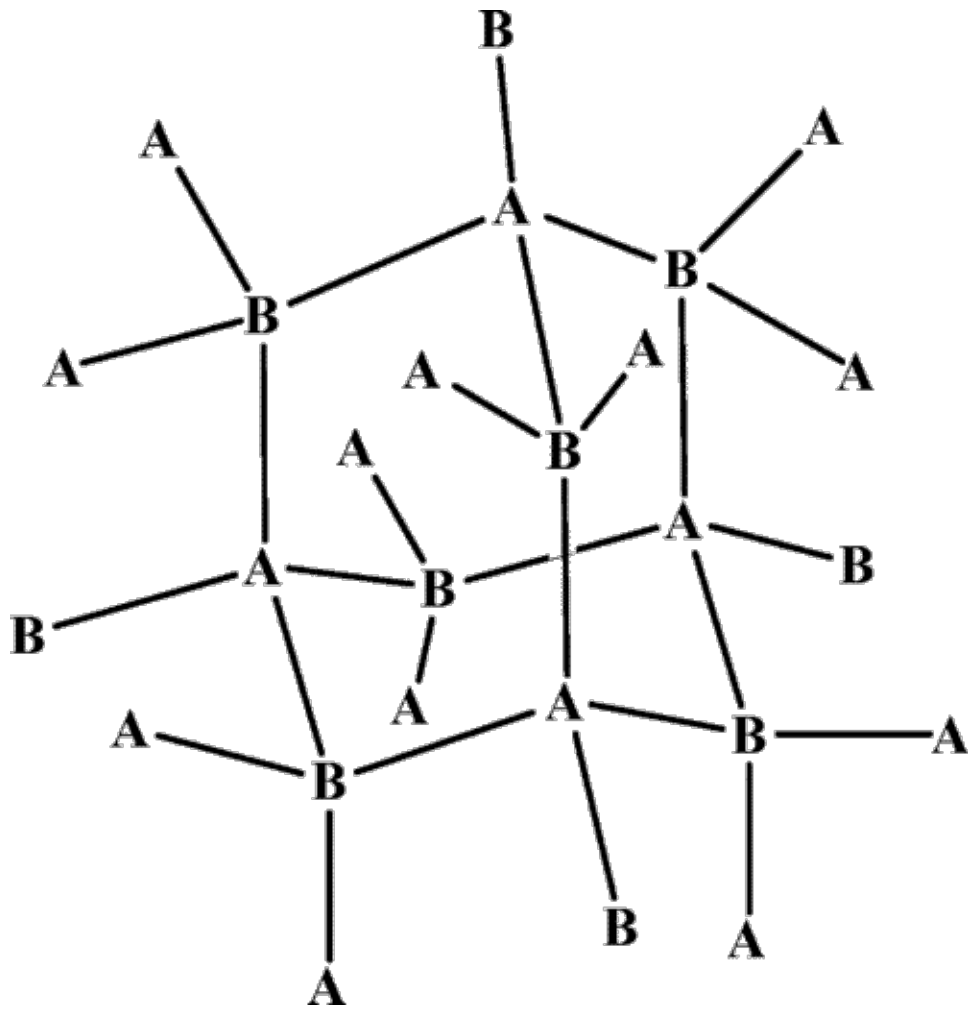


Chart 3

Although seemingly easy to assemble,<sup>15</sup> the majority of the diamondoid networks suffer from severe instability because of their loose packing. All of these structures inherently contain cavities in which the (large) size is determined by the distance between tetrahedral nodes. The close-packing principle can normally be satisfied only for the most simple diamondoid structures such as elemental silicon, germanium, gray tin, zinc blende, etc. Yet for diamondoid motifs built of the more extended elements, the void space within the adamantane cages can be quite significant and constitute more than 50% of the overall structural volume. Without extra supporting features, such superporous structures generally suffer from shakiness and are prone to collapse easily.<sup>16</sup>

An innate solution of the void problem lies in the spontaneous formation of not one, but several identical diamondoid networks that interpenetrate and thus provide the appropriate packing density. This structural phenomenon has been found to be of general importance for three-dimensional networks,<sup>17</sup> and, in particular, the geometrical conditions of the interpenetration have been explicitly formulated for diamondoid networks.<sup>18</sup> Another, more controllable, option for stabilizing large diamondoid networks can be found in the formation of clathrates.<sup>19</sup> Importantly, the generally unimpressive stability of clathrate systems can be dramatically improved by

strong Coulombic forces, when the neutral guest molecules are substituted by counterions of the appropriate size and the diamondoid network itself has the opposite electrical charge.<sup>21</sup>

To systematically develop the charge-transfer (CT) motif for the crystal engineering of stable diamondoid networks, we wish to now focus on the utilization of carbon tetrabromide ( $\text{CBr}_4$ ) as the simplest (tetrahedral) building element. Indeed, this prototypical electron acceptor forms intermolecular complexes with one-dimensional donors,<sup>24</sup> the charge-transfer nature of which has been revealed in a series of physical-chemical studies.<sup>25</sup> Although the isolation of crystalline solids met significant difficulties due to the relatively low free energy of the complex formation, we earlier found stronger charge-transfer complexes of  $\text{CBr}_4$  using better electron donors, especially tertiary aliphatic amines.<sup>26</sup> On the basis of that study, Desiraju and co-workers attempted an assembly of crystalline diamondoid donor/acceptor networks using hexamethylenetetramine (HMT) as the tetrahedral donor core.<sup>13a</sup> The resulting diamondoid (sphaleroid) network suffered from positional disorder between  $\text{CBr}_4$  and HMT (because of their similar size). A subsequent attempt to stabilize an extended tetrabromoadamantane/HMT network, using an excess of tetrahedral  $\text{CBr}_4$  to fill the cavities, resulted in a much weaker (and also disordered) donor/acceptor assembly.<sup>13b</sup> Additionally, these systems lacked continuous electronic coupling (i.e., through-orbital interaction) within their diamondoid networks because of the nonconducting nature of aliphatic  $\text{CH}_2$ -bridges in the HMT and (tetrabromo)adamantane units.

Our interest in electronically coupled<sup>27</sup> donor/acceptor diamondoid networks is based on the equimolar combination of the carbon tetrabromide acceptor with simple inorganic anionic donors, because the halide ions (chloride, bromide, and iodide) are known to form donor/acceptor complexes with  $\text{CBr}_4$ .<sup>28,29</sup> Importantly, the use of these electrically charged donor units provides us with four significant advantages: (a) the enhancement of the network-forming CT interactions, (b) the general structural stabilization due to formation of ionic “clathrate” networks where the appropriate packing density is additionally supported by Coulombic forces between “guest” cations and the embodying anionic “host” matrix, (c) the variable size of the countercation to allow a controlled adjustment of the packing density – the ready availability of a series of tetraalkylammonium ions ( $\text{NR}_4^+$ ) of progressively different sizes ( $\text{R} = \text{Me}, \text{Et}, \text{Pr}, \text{and Bu}$ ) being especially important, and (d) we believe the ( $\text{Br}_3\text{CBr}\cdots\text{halide}$ ) association represents quite a feasible combination for continuous electronic coupling throughout the entire donor/acceptor network. Finally, we stress that such a diamondoid design with the alternate donor/acceptor synthons leads to highly desirable acentric structures, because of the polar “sphaleroid” symmetry,<sup>14</sup> and these are known to produce crystals with nonlinear optical properties.<sup>12</sup>

## Results

Although there have been attempts to employ progressively weaker intermolecular interactions for the molecular crystal assembly of diamondoid networks,<sup>3,4,6,10</sup> such interactions must be sufficiently strong (and directional) to be dominant over other (offsetting) crystal packing forces. However, because of controversial estimates of the suitability

of carbon tetrabromide for use in stable crystalline (3-D) donor/acceptor assemblies,<sup>30</sup> our first goal was to evaluate quantitatively the nature and strength of the [1:1] association of CBr<sub>4</sub> with various halide anions, as well as the magnitude of the charge-transfer electronic coupling element between these acceptor/donor moieties via spectral measurements in solution.<sup>32</sup>

### I. Charge-Transfer Association of Carbon Tetrabromide and Halide Salts. A. Electronic (UV-Vis) Spectra of [1:1]

**CBr<sub>4</sub>/Halide Complexes.** When carbon tetrabromide ( $\lambda_{\max} = 225 \text{ nm}$ ,  $\epsilon_{225} = 6.2 \times 10^3 \text{ M}^{-1} \text{ cm}^{-1}$ ) was incrementally added to tetra-*n*-propylammonium bromide ( $\lambda_{\max} < 200 \text{ nm}$ ) in dichloromethane, a new, distinctive spectral band appeared and progressively grew at  $\lambda_{\max} = 292 \text{ nm}$  as illustrated in Figure 1. The application of Job's method<sup>33</sup> to the new absorbance at different molar ratios of CBr<sub>4</sub>/Br<sup>-</sup> confirmed the [1:1] stoichiometry of the electron donor/acceptor (EDA) association,<sup>34</sup> that is



Similar spectral behavior was observed for carbon tetrabromide with chloride and iodide as the *n*-propylammonium salts (see Table 1).<sup>35,36</sup>

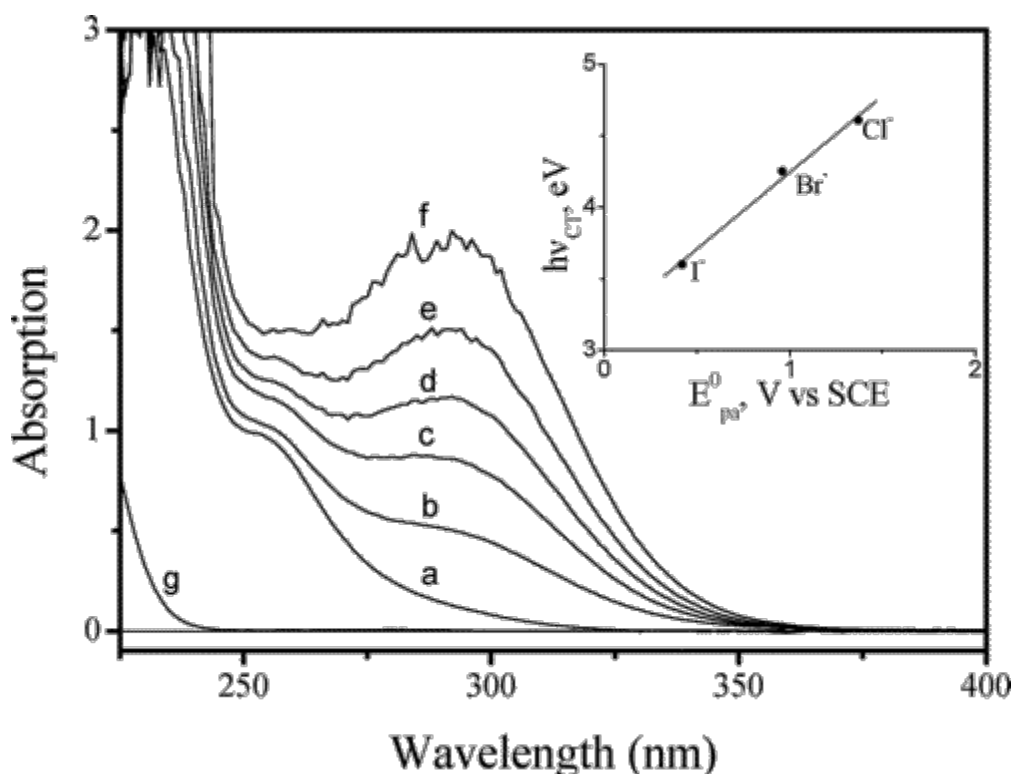


Figure 1 Spectral changes attendant upon the addition of tetrapropylammonium bromide to a 7.5 mM solution of carbon tetrabromide in dichloromethane at 22 °C. Concentration of Pr<sub>4</sub>N<sup>+</sup>Br<sup>-</sup> [mM]: (a) 0; (b) 18; (c) 38; (d) 56; (e) 75; (f) 94. For comparison: (g) is the spectrum of 50 mM Pr<sub>4</sub>N<sup>+</sup>Br<sup>-</sup> alone. Inset: Mulliken correlation between the energy of the charge-transfer band and the oxidation potential of the donor in the complexes of CBr<sub>4</sub> acceptor with halides (as indicated).

Table 1. Spectroscopic and Energetic Characteristics of the Charge-Transfer Complexes between CBr<sub>4</sub> and Halide Ions<sup>a</sup>

halide	Cl <sup>-</sup>	Br <sup>-</sup>	I <sup>-</sup>
$\lambda_{\max}$ [nm]	265	292	345

$\epsilon_{CT} [M^{-1}cm^{-1}, \times 10^{-4}]^b$	0.6	1.0	1.3
$K [M^{-1}]^c$	3.0	2.8	3.2
$E_{pa} [V, \text{vs SCE}]$	1.37	0.96	0.42
$R_{DA} [\text{\AA}]^d$	3.09	3.15	3.30
$H_{DA} [eV]$	0.62	0.65	0.54

<sup>a</sup> As  $NPr_4^+$  salts in dichloromethane solution at 22 °C. <sup>b</sup> Estimated standard deviation  $0.1 \times 10^4 M^{-1} cm^{-1}$ . <sup>c</sup> Estimated standard deviation  $0.5 M^{-1}$ . <sup>d</sup> The Br $\cdots$ halide separation was determined crystallographically.

**B. Mulliken Correlation of the Charge-Transfer Energies.** Although the halide association with carbon tetrabromide has been tentatively ascribed to an intermolecular donor/acceptor interaction,<sup>28c</sup> only electronic spectroscopy can provide the unambiguous assignment to the charge-transfer nature of the binding. Thus, according to Mulliken,<sup>37</sup> the energies ( $h\nu_{CT}$ ) of the absorption bands of a related series of molecular complexes sharing a common acceptor ( $CBr_4$ ) must be linearly dependent on the oxidation potentials of the donors (halides). The latter were quantitatively extracted as the cyclic voltammetric peak potentials ( $E_{pa}$ , V vs SCE) as listed in Table 1. The linear correlation in Figure 1 (inset) of these anodic potentials with the spectral energies of the chloride, bromide, and iodide complexes establishes the charge-transfer character of the  $CBr_4$ /halide associations.

**C. Charge-Transfer Bindings of Carbon Tetrabromide to Halide Donors.** The thermodynamics of the  $CBr_4$ /halide bindings in eq 1 were quantitatively calculated from the formation constants  $K_{EDA}$  according to the Benesi–Hildebrand methodology,<sup>38</sup> that is

$$\frac{[CBr_4]}{A_{CT}} = \frac{1}{\epsilon_{CT}} + \frac{1}{K_{EDA}\epsilon_{CT}[\text{halide}]} \quad (2)$$

where  $A_{CT}$  and  $\epsilon_{CT}$  are the absorbance and extinction coefficient of the new (charge-transfer) absorption band. Essentially the same values of the formation constants were independently obtained using the Drago procedure.<sup>33</sup> The resulting values of  $K_{EDA}$  in Table 1 lay in the rather narrow range of  $K_{EDA} = 2.8\text{--}3.2 M^{-1}$ , consistent with some earlier determinations.<sup>28a,32</sup> Indeed, such values represent free energies of formation of  $-\Delta G_{EDA} = 2.7$  (chloride), 2.5 (bromide), and 2.8 (iodide) kJ/mol and place this class of donor/acceptor interactions in the range of various other charge-transfer complexes for crystal-forming purposes.<sup>39</sup>

**D. Electronic (HOMO–LUMO) Coupling of Carbon Tetrabromide and Halide Moieties.** The discrete charge-transfer bands of the various  $CBr_4$ /halide complexes in Table 1 allow the effectiveness of the electronic coupling between the  $CBr_4$  acceptor and the halide donors to be quantitatively evaluated.<sup>37,40</sup> Thus, in charge-transfer complexes, the Mulliken–Hush theory predicts the electronic coupling element ( $H_{DA}$ ) between the donor and acceptor moieties to be directly related to the spectral properties and the structure of the complex as

$$H_{DA} = 0.0206(\nu_{CT}\Delta\nu_{1/2}\epsilon_{CT})^{1/2}/R_{DA} \quad (3)$$

where  $\nu_{CT}$ ,  $\Delta\nu_{1/2}$ , and  $\epsilon_{CT}$  are the energy of the spectral band, its full width at half-height (in eV), and the molar extinction coefficient (in  $M^{-1} cm^{-1}$ ), respectively.  $R_{DA}$  is the spatial separation ( $\text{\AA}$ ) between the donor/acceptor centers,



which we evaluated from the X-ray crystallographic results (vide infra). The sizable magnitudes of the values of  $H_{DA}$  in the range 0.5–0.6 eV for the various  $CBr_4$ /halide complexes in Table 1 are strongly indicative of the considerable orbital interaction (electronic coupling) that is extant in the  $CBr_4$ /halide system.<sup>41</sup>

Spectroscopic studies thus point to the binary association of  $CBr_4$  and either chloride, bromide, or iodide that is uniformly strong and appropriately accompanied by efficient electronic coupling and therefore suitable for the charge-transfer assembly of diamondoid (electronically coupled) networks. A variety of crystalline [1:1] complexes of the general formula  $[R_4N^+ \text{halide}^-, CBr_4]$  can be easily and regularly prepared in different nonaqueous solutions by merely mixing equimolar amounts of the constituents.<sup>28a,b</sup> The fact that such a highly heteropolar mixture of an (ionic) salt and neutral (uncharged) acceptor would so readily yield true charge-transfer complexes is by itself rather unusual, because it is much more common to experience their separate crystallization as a mixture of homoseric crystals. As a result, we could examine two series of charge-transfer crystals to monitor the structural changes arising from (a) the nature of the halide donor and (b) the size of the tetraalkylammonium counterion as follows.

**II. X-ray Crystallography of Charge-Transfer Complexes of Carbon Tetrabromide with Alkylammonium Halides. A. Effect of Halide Variation.** The graded series of the diamondoid donor/acceptor network shown in Figure 2 derive from the charge-transfer complexes of tetraethylammonium salts with the halide as chloride, bromide, and iodide, in which the tetrahedral  $CBr_4$  alternates in a regular manner with the halide at the nodes of adamantane-like cages. The general shape of the cages, secluded for scrutiny in Figure 3, is identical for all three isomorphous structures, but their size depends on the “length” of the  $(Br_3CBr \cdots \text{halide})$  interaction. The smallest chloride donor gives  $Br \cdots Cl^-$  distances of 3.090 Å (shortened by 0.51 Å from the van der Waals limit<sup>31</sup>) and a cage volume of 392.8 Å<sup>3</sup>. The midsize bromide gives  $Br \cdots Br^-$  distances of 3.154 Å (shortened by 0.55 Å from the van der Waals limit<sup>31</sup>) and a cage volume of 407.3 Å<sup>3</sup>. Finally, the largest iodide gives  $Br \cdots I^-$  distances of 3.298 Å (shortened by 0.53 Å from the van der Waals limit<sup>31</sup>) and a cage volume of 443.5 Å<sup>3</sup>.

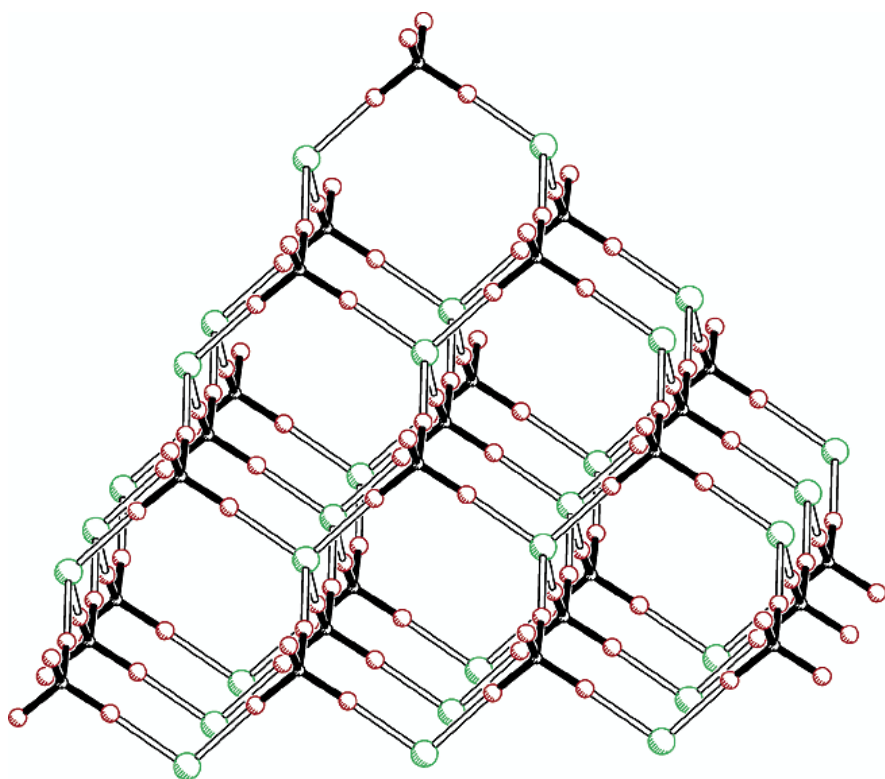


Figure 2 The diamondoid donor/acceptor network in the structures of  $[\text{Et}_4\text{N}^+\text{halide}^-\text{,CBr}_4]$  complexes. In all figures, the halide anions are shown as green circles, and the donor/acceptor bonds are shown as empty lines. The  $\text{Et}_4\text{N}^+$  counterions are omitted for clarity.

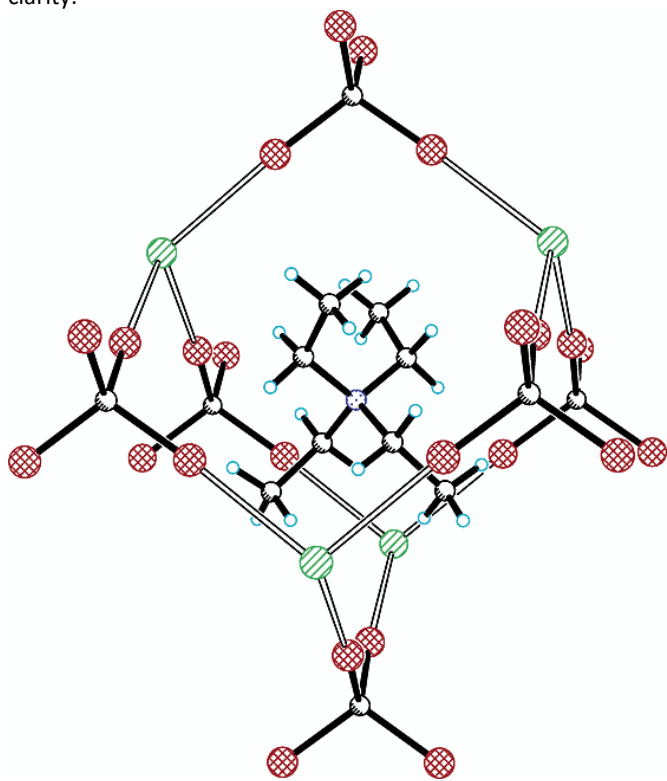


Figure 3 The elementary adamantane-like cage in the structures of  $[\text{Et}_4\text{N}^+\text{halide}^-\text{,CBr}_4]$  complexes supported from within the cavity by  $\text{NEt}_4^+$  counterion.

The significant change of the cell volume (by 13%) in proceeding from chloride to iodide is accommodated by the  $\text{Et}_4\text{N}^+$  counterions, which support the lacelike anionic diamondoid constructions from within their cavities. It is important to mention that these diamondoid structures of the spheroid structural class contain adamantane-like cavities of two different types,  $\text{A}_4\text{D}_6$  and  $\text{A}_6\text{D}_4$  ( $\text{A} = \text{CBr}_4$  and  $\text{D} = \text{halide}$ ), where the “tetrahedral” and “octahedral” vertices are occupied by different components as is schematically illustrated in Chart 4. Generally speaking, the electrostatic potential within these two types of cavities is different, and they are structurally nonequivalent, the  $\text{Et}_4\text{N}^+$  ion being found only in the  $(\text{CBr}_4)_6(\text{halide})_4$  cavity (see Figure 3).<sup>42</sup> Simultaneously, the terminal ethyl arms of the counteranion interpenetrate from four sides into the adjacent  $(\text{CBr}_4)_4(\text{halide})_6$  cavities to effectively fill the void space. As a result, the  $(\text{CBr}_4)_4(\text{halide})_6$  cavities are occupied by quartets of the closely packed Me-groups making van der Waals contacts with each other. In the rather expanded iodide structure, the loose fitting of the  $\text{Et}_4\text{N}^+$  ions is characterized by rotational disorder.

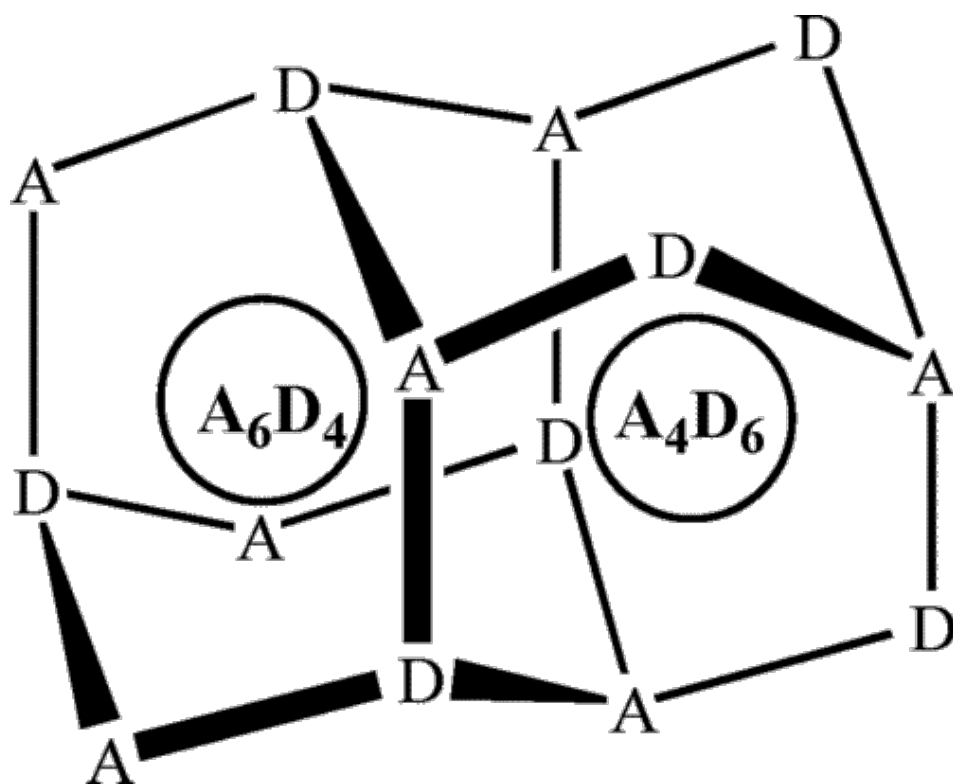


Chart 4

All of the tetraethylammonium complexes crystallize in the space group of symmetry  $I-4$  that reflects the predictable absence of inversion centers in such alternated donor/acceptor diamondoid networks (Figure 3).<sup>43</sup> However, none of the charge-transfer crystals have an ideal (diamondoid) F-centered cubic symmetry.<sup>44</sup> The reason for the observed tetragonal distortions can be attributed to the shape of the tetraethylammonium cations, which are deprived of three-fold symmetry and thus cannot fit ideally into a cubic crystal arrangement.<sup>45</sup> Importantly, such tetragonal deviations from cubic symmetry are known to enhance nonlinear optical properties of some diamondoid inorganic structures.<sup>12b</sup>

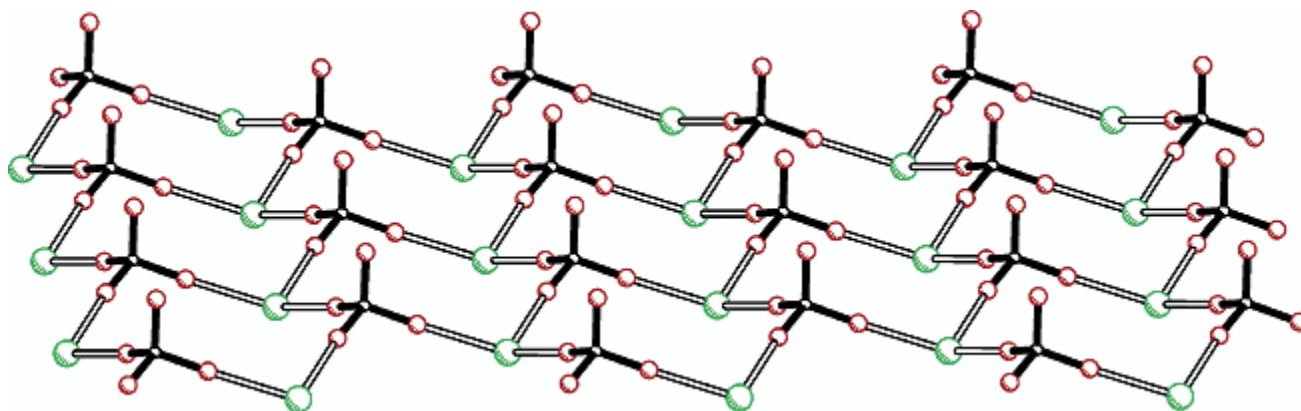


Figure 4 The two-dimensional honeycombed donor/acceptor layer in the structure of  $[\text{Bu}_4\text{N}^+\text{Br}^-\cdot\text{CBr}_4]$  as the result of fragmentation of the three-dimensional diamondoid network shown in Figure 2. Note: the noncentrosymmetric structure is polarized across the mean plane.

**B. Effect of Counterion Variation.** The variations in the size of the “supporting” tetraalkylammonium counterions were expected to modify, or even break, the diamondoid connectivity of the donor/acceptor moieties in the  $\text{CBr}_4$ /halide networks.<sup>46</sup> Even if the precise outcome of this modification was difficult to predict, the experimentally obtained crystal structures could be rationalized remarkably well for those derived from the charge-transfer complexes  $[\text{NMe}_4^+\text{Br}^-\cdot 2\text{CBr}_4]$ ,  $[\text{NPr}_4^+\text{Br}^-\cdot\text{CBr}_4]$ ,  $[\text{NBu}_4^+\text{Br}^-\cdot\text{CBr}_4]$ , and  $[\text{DBU}-\text{H}^+\text{Br}^-\cdot\text{CBr}_4]$ ,<sup>47</sup> as follows:

(i) The smallest size of the  $\text{Me}_4\text{N}^+$  cation was not sufficient to support the integrity of the diamondoid network, although it was envisaged<sup>28a,b</sup> that the developing voids could be filled with additional  $\text{CBr}_4$  acceptor. Indeed, the [1:2] complex  $[\text{NMe}_4^+\text{Br}^-\cdot 2\text{CBr}_4]$  that precipitated from solution contained an additional molecular equivalent of  $\text{CBr}_4$  to maintain the diamondoid arrangement and (primitive) cell dimensions quite similar to that of its  $\text{Et}_4\text{N}^+$  analogue.<sup>48</sup>

(ii) With a tetraalkylammonium ion of a larger size than  $\text{Et}_4\text{N}^+$ , a fragmentation of the pristine diamondoid network was likely to occur as a result of the internal (steric) obstacles. Remarkably, we found the structure of tetrabutylammonium derivative to result in a two-dimensional donor/acceptor grid (Figure 4) that continues to mimic the structure of the original diamondoid network. These fragments represent the exact replica of slices taken across three-fold “cubic” axes of the original diamondoid network (cf. Figure 2), and they are separated by layers of tetrabutylammonium ions and acetone solvate (see Figure S1 in the Supporting Information).

Topologically, these grids are built of a number of trans-fused “cyclohexane” rings, in which each donor and acceptor unit has its coordination number reduced from 4 to 3. [These trans-fused layers are topologically similar to those found in the structure of rhombohedral black phosphorus as well as the common allotropes of As, Sb, and Bi.] The  $(\text{CBr}\cdots\text{Br})$  distances of 3.252–3.282 Å are slightly longer than those in the corresponding diamondoid network. Importantly, the uncoordinated C–Br bonds of the  $\text{CBr}_4$  acceptor and the “unused” electron pairs of bromide ions are oriented in mutually opposite directions. These result in the polarization of such noncentrosymmetric layers in the direction perpendicular to their planes and lead to the acentric symmetry of the entire crystal (space group of symmetry  $P2_1$ ).

(iii) Crystallization of the  $\text{Pr}_4\text{N}^+$  salt resulted in a different, but topologically closely related, two-dimensional pattern illustrated in Figure 5.

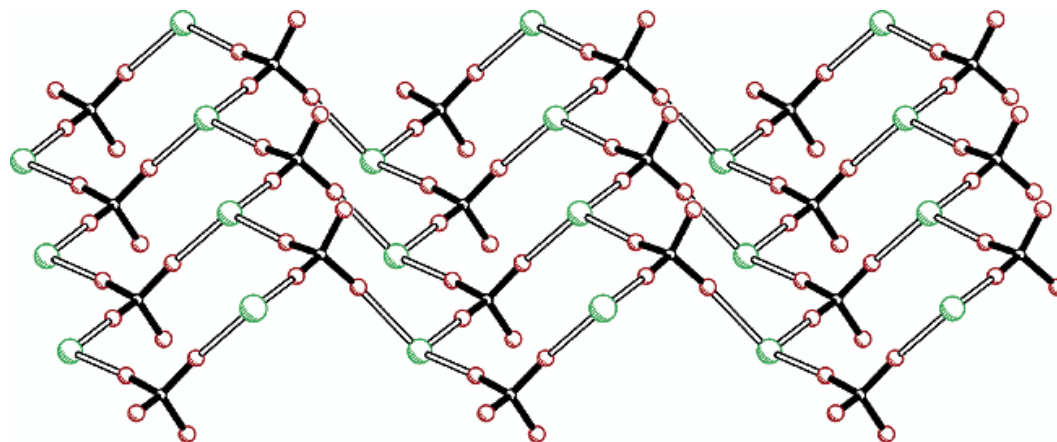


Figure 5 The two-dimensional folded donor/acceptor layer in the structure of  $[\text{Pr}_4\text{N}^+\text{Br}^-\text{CBr}_4]$  as the product of the rearrangement of the two-dimensional “diamondoid” layer in Figure 4. Note: the noncentrosymmetric structure is polarized along the mean plane.

The grid is also built of a number of “cyclohexane” units with the rings trans- and cis-fused in two mutually orthogonal directions. This results in a more folded shape of the layers, but with the coordination geometry of  $\text{CBr}_4$  and bromide remaining exactly the same as those in the related  $\text{Bu}_4\text{N}^+$  structure. [These folded two-dimensional layers topologically relate to those found in the structure of orthorhombic black phosphorus.] The ( $\text{CBr}\cdots\text{Br}$ ) distances show a somewhat larger variation that lies within the range of 3.19–3.31 Å. The folded layers are also deprived of inversion centers, but they are polarized along their mean planes. The alternation of the layers of opposite polarity along the crystal results in its overall centric symmetry (see Figure S2 in the Supporting Information).

(iv) The (tetrahedral) coordination geometry of both the donor (halide) and the acceptor ( $\text{CBr}_4$ ) components remains very conservative in all of the charge-transfer complexes, and they always attain the maximum possible coordination number. These structural features persist even in the presence of other dominant intermolecular forces such as the relatively strong hydrogen bonds  $\text{N}^+\text{--H}\cdots\text{Br}$  ( $\text{H}\cdots\text{Br}$  2.65 Å) in the structure of the secondary ammonium complex  $[\text{DBU--H}^+\text{Br}^-\text{CBr}_4]$  (see Figure S3 in the Supporting Information). Despite this strongly perturbing structural factor, the coordination geometry and coordination numbers of the  $\text{CBr}_4$  and  $\text{Br}^-$  units remain the same as those in the previous structures with  $\text{Br}\cdots\text{Br}$  distances of 3.260–3.375 Å and  $\text{C--Br}\cdots\text{Br}$  angles of 164.2–172.5°. However, some excessive angular distortions around bromide anions produce a new pattern for the donor/acceptor two-dimensional grids, which consist of the trans-cis-fused “cyclooctane” and “cyclobutane” rings (Figure 6). The shapes of these rings permit inversion centers, and the entire structure is centrosymmetric.

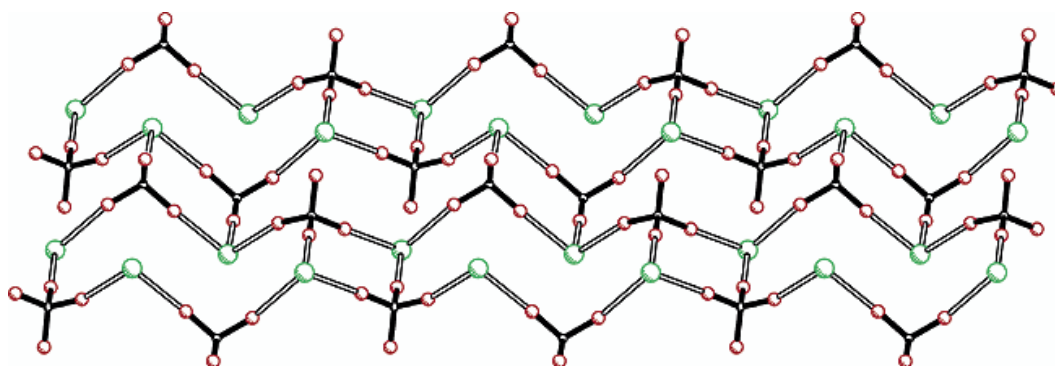


Figure 6 The two-dimensional centrosymmetric donor/acceptor layer in the structure of [DBU-H<sup>+</sup>Br<sup>-</sup>,CBr<sub>4</sub>] distorted by competition with H-bonding in the crystal, see text.

## Discussion

Spectroscopic studies of electron donor/acceptor dyads (in solution) establish the significant strengths of the intermolecular (Br<sub>3</sub>CBr⋯halide) interactions, which are consonant with their importance in structural manifestations for crystal engineering. Such charge-transfer interactions are characterized by measurable shortenings of the interhalogen (CBr⋯halide) distances by 0.50–0.55 Å relative to standard van der Waals separations,<sup>31</sup> and this is accompanied by the elongation of the (C–Br) σ-bond by ~0.025 Å as compared to that in the uncoordinated CBr<sub>4</sub> acceptor,<sup>49</sup> both in accord with the p-σ\* nature of the orbital (HOMO–LUMO) interaction according to Mulliken theory.<sup>37</sup>

The strict directional character of the (Br<sub>3</sub>CBr⋯halide) interaction is illustrated by the uniformly invariant angles of  $\theta = 175.0\text{--}176.5^\circ$  for the (CBr⋯halide) ensembles in the diamondoid networks for the series [Et<sub>4</sub>N<sup>+</sup>halide,CBr<sub>4</sub>], and  $\theta = 164.6\text{--}177.1^\circ$  in the more distorted “sliced” networks in [Pr<sub>4</sub>N<sup>+</sup>Br<sup>-</sup>,CBr<sub>4</sub>] and [Bu<sub>4</sub>N<sup>+</sup>Br<sup>-</sup>,CBr<sub>4</sub>]. Moreover, the tetrahedral coordination of the CBr<sub>4</sub> moieties is unperturbed, with the internal (Br–C–Br) bond angle being close to the ideal value of  $\theta = 109.4^\circ$  in all of these charge-transfer crystals. The intermolecular (Br⋯halide⋯Br) angles lie within the range  $\theta = 101.5\text{--}113.6^\circ$  in the diamondoid structures of [Et<sub>4</sub>N<sup>+</sup>halide,CBr<sub>4</sub>] and are only somewhat more distorted ( $97.0\text{--}126.2^\circ$ ) in the coordinationally “unsaturated” structures of [Pr<sub>4</sub>N<sup>+</sup>Br<sup>-</sup>,CBr<sub>4</sub>] and [Bu<sub>4</sub>N<sup>+</sup>Br<sup>-</sup>,CBr<sub>4</sub>].

The strength and directionality of the intermolecular (Br<sub>3</sub>CBr⋯halide) interactions together are important prerequisites for use in supramolecular designs, and this donor/acceptor aggregation is persistent throughout all of the charge-transfer complexes examined in this study, resulting in quite similar structural patterns. Even in the case (reported earlier<sup>29</sup>) in which severe steric hindrance was imposed by bulky (Ph<sub>4</sub>P<sup>+</sup>) counterions, the charge-transfer (Br<sub>3</sub>CBr⋯Br) association is the dominant feature of the crystal structure.<sup>46</sup> Furthermore, in the presence of the protonated amine (DBU–H<sup>+</sup>) prone to the formation of strong (N<sup>+</sup>H⋯Br) hydrogen bonds, the same charge-transfer association prevails (see Figure S3 in the Supporting Information). Indeed, such observations lead to our conclusion that the structure-forming capability of the (Br<sub>3</sub>CBr⋯halide) interactions is comparable to, or even greater than, that possessed by (regular) hydrogen bonds.

As a structurally simple and compact acceptor, carbon tetrabromide is an attractive core for the building of novel three-dimensional (crystal) structures akin to those constructed earlier with other types of tetrahedral building blocks.<sup>1-11</sup> In particular, the use of various tetraalkylammonium halides as the electron-donor components bypasses the conventional problem usually encountered in dealing with the stability issue imposed by large (adamantane-shaped) internal cavities inherent to such diamondoid networks.<sup>16</sup> Most importantly, the incorporation of the tetraethylammonium cation leads to optimal support of the diamondoid network (Figure 2) of CBr<sub>4</sub> and halide by stabilizing the cavity void (Figure 3). Cations of larger size fragment these networks into two-dimensional “slices” (Figures 4 and 5), but the sizes of Pr<sub>4</sub>N<sup>+</sup> and Bu<sub>4</sub>N<sup>+</sup> are not yet significant to fill the separations between the resulting charge-transfer grids. As a result, the layers in the Pr<sub>4</sub>N<sup>+</sup> structure collapse toward each other to accept a crimped structure and induce short interlayer (Br...Br) contacts of 3.35 Å (see Figure S2 in the Supporting Information). In the largest Bu<sub>4</sub>N<sup>+</sup> structure, the undistorted diamondoid slices require the intercalation of both the cation as well as an additional (acetone) solvate. At the other extreme, the stabilization of the diamondoid core in the smallest Me<sub>4</sub>N<sup>+</sup> structure requires an additional equivalent of carbon tetrabromide for filling the voids.

In addition to the structural integrity of such electron donor/acceptor networks in crystal engineering, two other factors are critical to their transformation into useful materials. First, the symmetry factor refers to the absence of inversion centers for certain types of supramolecular (diamondoid) networks, because many useful properties arise from the crystal acentricity, especially for the second-order hyperpolarizability.<sup>51</sup> Second, the electronic factor refers to the effective communication between the nodes of the diamondoid nets.<sup>52</sup> Indeed, the charge-transfer complexes of carbon tetrabromide and alkylammonium halides satisfy (in measure) both of these rather stringent requirements by yielding robust charge-transfer crystals that (a) belong to the sphaleroid structural class deprived of inversion centers and (b) possess substantial electron coupling ( $H_{DA}$  in Table 1) between donor/acceptor centers.

## Summary and Conclusions

Carbon tetrabromide spontaneously forms a series of intermolecular complexes with electron-rich halide anions (chloride, bromide, and iodide) that are characterized by the unusual strength and directionality as well as large electronic (HOMO–LUMO) couplings of the halide donor and CBr<sub>4</sub> acceptor. Spectral (UV–vis) studies in solution establish the charge-transfer nature of the (CBr<sub>4</sub>/halide) interactions, and these combined with the tetrahedral shape of the acceptor lead to supramolecular (crystalline) assemblies of advanced 3-D (diamondoid) networks that are uniquely stabilized by the proper choice of tetraalkylammonium counterions to fill the adamantanoid cavities. Most importantly, the alternate population of the diamondoid nodes, consisting of contiguous donor (halide) and acceptor (CBr<sub>4</sub>) units, effectively results in the annihilation of inversion centers of symmetry, in agreement with the sphaleroid structural subclass.

As we already cited, the sphaleroid structure of the subject complexes is closely related to the structure of inorganic binary compounds known for their nonlinear optical properties.<sup>12</sup> Indeed, there were already some deliberate attempts to utilize organic (diamondoid) networks for the SHG-active crystal designs,<sup>9d</sup> and thus the charge-transfer



nature of (CBr<sub>4</sub>,halide) complexes represents a factor potentially favorable for high second-order hyperpolarizability.<sup>27,55</sup> These considerations encouraged us to submit samples of the noncentrosymmetric complexes [Et<sub>4</sub>N<sup>+</sup>Cl<sup>-</sup>,CBr<sub>4</sub>], [Et<sub>4</sub>N<sup>+</sup>Br<sup>-</sup>,CBr<sub>4</sub>], and [NBu<sub>4</sub><sup>+</sup>Br<sup>-</sup>,CBr<sub>4</sub>] to a specialized research facility for evaluation. Preliminary results show all of these diamondoid charge-transfer associates to possess unusual nonlinear optical properties; the intensity of SHG was found to be qualitatively comparable to that of the best inorganic (LiNbO<sub>3</sub>) or organic (urea) materials.<sup>56</sup> We are open to extensive collaborative studies that will provide further quantitative validation and thus lead to new designs of acentric diamondoid networks.

## Experimental Section

**Materials.** Carbon tetrabromide, tetraethylammonium chloride, bromide, and iodide, tetrapropylammonium chloride, bromide, and iodide, tetrabutylammonium bromide, and 1-aza-8-azoniabicyclo(5.4.0)undec-7-ene bromide from Aldrich were used without further purification. Dichloromethane, acetone, and acetonitrile from Merck were purified according to standard laboratory procedures<sup>57</sup> and were stored in Schlenk flasks under an argon atmosphere.

**Measurements of the Charge-Transfer Spectra of [CBr<sub>4</sub>,Halide] Complexes.** All spectroscopic measurements were performed in a 1 mm quartz cuvette on a Hewlett-Packard 8453 diode-array UV-vis spectrometer. Freshly prepared stock solutions of carbon tetrabromide and alkylammonium salts of halide ions were used. Measurements were carried out under air (the complex formation of carbon tetrabromide with iodide ions was studied under protection from adventitious light because ambient light irradiation resulted in the formation of I<sub>2</sub> and I<sub>3</sub>; in other cases, no special precautions were taken).

The incremental addition of alkylammonium halide salts to the CBr<sub>4</sub> solution resulted in the appearance of new bands (see Figure 1) at 300 ± 50 nm. Because of the partial overlap of the new absorption bands with the tail of absorption of CBr<sub>4</sub> (for the systems with bromide and especially chloride ions), the accurate spectral characteristics of these bands were obtained by digital subtractions of CBr<sub>4</sub> spectrum from the spectra of CBr<sub>4</sub>/halide mixtures. [Carbon tetrabromide has an absorption band at λ<sub>max</sub> = 225 nm with ε<sub>max</sub> = 6.2 × 10<sup>3</sup> mol<sup>-1</sup> cm<sup>-1</sup> and a shoulder at λ<sub>sh</sub> = 255 nm; tetrapropylammonium iodide has λ<sub>max</sub> = 245 nm with ε<sub>max</sub> = 1.7 × 10<sup>4</sup> mol<sup>-1</sup> cm<sup>-1</sup>; tetrapropylammonium chloride and tetrapropylammonium bromide do not have any absorption maxima beyond 220 nm.] To determine the stoichiometry of the complexes formed, the stock solutions of the donor and acceptor with the same concentration (18 mM) were mixed in ratios varying from 10:1 to 1:10 (Job's method<sup>33</sup>). The maximal absorption intensity of the new CT band was observed when the concentrations of the reagents were equal, indicating that CBr<sub>4</sub> forms 1:1 complexes with halide ions in solutions.<sup>34</sup> To determine formation constants K<sub>EDA</sub> and the molar absorption coefficients ε<sub>CT</sub> of various [CBr<sub>4</sub>,halide] complexes, the stock solutions of the reagents were mixed so that the concentration of the acceptor (CBr<sub>4</sub>) was kept constant (5–10 mM) throughout a series of measurements, while the concentration of the donor (halide) was incrementally increased (from 10 to 1000 mM). The measured intensities of the CT bands were treated according to the Benesi-Hildebrand procedure in eq 2.<sup>38</sup> The plot of [CBr<sub>4</sub>]/A<sub>CT</sub> versus reciprocal concentration of added halide was linear, and the least-squares fit yielded a correlation coefficient of greater than 0.99. From the



slope and the intercept, the values of  $K$  and  $\epsilon_{CT}$  were obtained. These parameters were also obtained via the treatment of the CT absorption data with the Drago procedure from the intersection of the  $K^{-1}$  versus  $\epsilon_{CT}$  dependencies plotted for several sets of initial concentrations of the reagents.<sup>33</sup> Thus, the  $K$  and  $\epsilon_{CT}$  in Table 1 represent the average values obtained using both (Benesi–Hildebrand and Drago) methods from three to four series of measurements for each of the donor/acceptor dyads.

Table 2. Crystallographic Parameters and the Details of the Structure Refinements

compound	NEt <sub>4</sub> Cl·CBr <sub>4</sub>	NEt <sub>4</sub> Br·CBr <sub>4</sub>	NEt <sub>4</sub> I·CBr <sub>4</sub>	NMe <sub>4</sub> Br· 2CBr <sub>4</sub>	NMe <sub>4</sub> I· 2CBr <sub>4</sub>	NPr <sub>4</sub> Br·CBr <sub>4</sub>	NBu <sub>4</sub> Br·CBr <sub>4</sub> · C <sub>3</sub> H <sub>6</sub> O	DABU–H <sup>+</sup> · CBr <sub>4</sub>	CBr <sub>4</sub>
formula	C <sub>9</sub> H <sub>20</sub> Br <sub>4</sub> ClN	C <sub>9</sub> H <sub>20</sub> Br <sub>5</sub> N	C <sub>9</sub> H <sub>20</sub> Br <sub>4</sub> IN	C <sub>6</sub> H <sub>12</sub> Br <sub>9</sub> N	C <sub>6</sub> H <sub>12</sub> Br <sub>8</sub> IN	C <sub>13</sub> H <sub>28</sub> Br <sub>5</sub> N	C <sub>20</sub> H <sub>42</sub> Br <sub>5</sub> NO	C <sub>10</sub> H <sub>17</sub> Br <sub>5</sub> N <sub>2</sub>	CBr <sub>4</sub>
$M$	497.35	541.81	588.80	817.36	864.35	597.91	712.10	564.81	331.65
space group	<i>I</i> -4	<i>I</i> -4	<i>I</i> -4	<i>Fm</i> -3 <i>m</i>	<i>Fm</i> -3 <i>m</i>	<i>P2</i> <sub>1</sub> / <i>n</i>	<i>P2</i> <sub>1</sub>	<i>P2</i> <sub>1</sub> / <i>c</i>	<i>C2</i> / <i>c</i>
$a$ [Å]	8.0215(1)	8.0992(3)	8.2859(1)	12.1850(3)	12.398(1)	8.4857(1)	8.2859(1)	7.6795(1)	21.086(2)
$b$ [Å]	8.0215(1)	8.0992(3)	8.2859(1)	12.1850(3)	12.398(1)	18.7993(3)	22.4833(4)	12.9359(1)	11.883(1)
$c$ [Å]	12.2085(2)	12.4173(5)	12.9194(1)	12.1850(3)	12.398(1)	13.0299(3)	8.3652(1)	16.5349(1)	20.674(2)
$\beta$ [deg]	90	90	90	90	90	99.992(1)	114.661(1)	101.481(1)	111.38(1)
$V$ [Å <sup>3</sup> ]	785.55(2)	814.54(5)	887.00(2)	1809.2(1)	1905.7(4)	2047.07(6)	1416.25(3)	1609.73(3)	4823.7(7)
$Z$	2	2	2	4	4	4	2	4	32
$D_c$ [g cm <sup>-3</sup> ]	2.103	2.209	2.205	3.001	3.013	1.940	1.670	2.331	3.653
$N_{ref}$ (collected)	5084	5125	5723	4886	925	25 640	18 190	11 372	24 064
$R_{int}$	0.0625	0.0252	0.0314	0.0270	0.0191	0.0436	0.0497	0.0269	0.0611
$N_{ref}$ (ind.)	1820	984	2037	194	201	9344	10 360	6050	7713
$N_{ref}$ [ $I > 2\sigma(I)$ ]	1648	971	1930	183	195	6455	8860	4874	4683
$R_1$	0.0365	0.0261	0.0414	0.0169	0.0201	0.0459	0.0438	0.0322	0.0431
$wR_2$	0.0825	0.0642	0.0922	0.0427	0.0527	0.0747	0.0945	0.0652	0.0959
Flack parameter	0.10(2)	0.5 <sup>a</sup>	0.15(2)	n/a	n/a	n/a	0.01(1)	n/a	n/a

<sup>a</sup> Regular twin, Friedel equivalents were averaged.

**Electrochemical Measurements.** Cyclic voltammetry (CV) was performed on a BAS 100A Electrochemical Analyzer. The measurements were carried out in a 4 mM alkylammonium halide solution in dry dichloromethane with 0.1 M supporting electrolyte (NBu<sub>4</sub><sup>+</sup>PF<sub>6</sub><sup>-</sup>) under argon atmosphere. All cyclic voltammograms were measured at the same sweep rate of 100 mV s<sup>-1</sup> with  $iR$  compensation. The working electrode consisted of an adjustable platinum disk with a surface area of ca. 1 mm<sup>2</sup>. The counterelectrode consisted of a platinum gauze that was separated from the working electrode by ca. 3 mm. The saturated calomel electrode (SCE) and its salt bridge were separated from the working electrode by a sintered glass frit. Because of the high reactivities of the halogen radicals, the reversible oxidation potentials of halide ions are not accessible. Instead, we have used irreversible anodic oxidation potentials,  $E_{pa}$ , readily obtained from the cyclic voltammograms ( $E_{pa} = 0.42, 0.96, \text{ and } 1.37 \text{ V vs SCE for I}^-, \text{ Br}^-, \text{ and Cl}^-, \text{ respectively}$ ).<sup>58</sup> Although these  $E_{pa}$  values contain contributions from kinetic terms ( $E^\circ = \beta E_{pa} + \text{const.}$ ), they provide the reliable relative values of oxidation potentials in a series of chemically similar donors (such as halide ions),<sup>59</sup> which can be used in various correlations.

**Mulliken–Hush Calculations of the Electronic Coupling Element  $H_{DA}$ .** The electronic coupling element,  $H_{DA}$ , representing the electronic (coupling) interaction between the donor and acceptor in the charge-transfer complex, was evaluated experimentally from the spectral data using the Mulliken–Hush methodology expressed in eq 3.<sup>37,40</sup> The values of  $v_{CT}$  and  $\Delta v_{CT}$  for the  $H_{DA}$  calculation were obtained by Gaussian deconvolution of the corresponding charge-transfer bands using Microcal Origin 6.0 program. The shortest distances between halide ions and bromine atoms in  $CBr_4$  determined from X-ray crystallographic data were used as the separation parameter  $R_{DA}$ .

**X-ray Crystallography.** The single crystals of the complexes were readily obtained by slow evaporation of the corresponding saturated equimolar acetone solutions in the air. The intensity data for all of the compounds were collected with the aid of a Siemens/Bruker SMART diffractometer equipped with a 1K CCD detector using Mo  $K_\alpha$  radiation ( $\lambda = 0.71073 \text{ \AA}$ ), at  $-150 \text{ }^\circ\text{C}$ . In all cases, the semiempirical absorption correction was applied.<sup>60</sup> The structures were solved by direct methods<sup>61</sup> and refined by a full matrix least-squares procedure<sup>62</sup> with IBM Pentium and SGI O<sub>2</sub> computers (see Table 2). [The X-ray structure details of various compounds are on deposit and can be obtained from the Cambridge Crystallographic Data Center, U.K.]

**Second Harmonic Measurements.** The Kurtz technique<sup>63</sup> was applied to measure the nonlinear optical response for the powder samples of the crystallographically noncentrosymmetric  $[\text{Et}_4\text{N}^+\text{Cl}^-\text{CBr}_4]$ ,  $[\text{Et}_4\text{N}^+\text{Br}^-\text{CBr}_4]$ , and  $[\text{Bu}_4\text{N}^+\text{Br}^-\text{CBr}_4, \text{C}_3\text{H}_6\text{O}]$ . Green second harmonic signals ( $\lambda_{SH} = 532 \text{ nm}$ ) were induced by a 1 Hz Q-switched Nd:YAG laser ( $\lambda_0 = 1064 \text{ nm}$ , power output 10 mJ in 7 ns pulse). The elliptic mirror was set up, with the sample in the primary focus and the detector (Hamamatsu HC-120 photomultiplier assembly) in the secondary focus. The SH signals were averaged by a digital storage scope to suppress noise. The samples of  $[\text{Et}_4\text{N}^+\text{Br}^-\text{CBr}_4]$ <sup>64</sup> were tested through a series of powders with particle sizes ranging from 20 to 90  $\mu\text{m}$  and loaded in glass ampules with 1 mm diameter. The  $P(2\omega)/P^2(\omega)$  second harmonic square dependence was obtained for the complexes and compared to that of the reference compound (quartz). The results characterize crystalline  $[\text{Et}_4\text{N}^+\text{Br}^-\text{CBr}_4]$  as a phase-matchable material. Anal. Calcd for  $\text{C}_9\text{H}_{20}\text{Br}_5\text{N}$ : C, 19.95; H, 3.72; N, 2.59. Found: C, 20.51; H, 3.83; N, 2.64 (Atlantic Microlab, Inc., Norcross, GA).

## Acknowledgment

We thank Y. S. Rosokha for the spectroscopic measurements and S. V. Rosokha for assistance with the computations and helpful discussions. We acknowledge the generous contribution of K. M. Ok and P. S. Halasyamani in kindly providing the (preliminary) second harmonics generation measurements. We also thank the National Science Foundation and the Robert A. Welch Foundation for financial support.

## References

- <sup>1</sup>(a) Ermer, O. *J. Am. Chem. Soc.* **1988**, *110*, 3747. (b) Ermer, O.; Eling, A. *Angew. Chem., Int. Ed. Engl.* **1988**, *27*, 829. (c) Ermer, O.; Lindenberg, L. *Helv. Chim. Acta* **1988**, *71*, 1084. See also: (d) Ermer, O.; Lindenberg, L. *Helv. Chim. Acta* **1991**, *74*, 825.
- <sup>2</sup>Simard, M.; Su, D.; Wuest, J. D. *J. Am. Chem. Soc.* **1991**, *113*, 4696.
- <sup>3</sup>Reddy, D. S.; Craig, D. C.; Desiraju, G. R. *J. Am. Chem. Soc.* **1996**, *118*, 4090.

- <sup>4</sup>(a) Galoppini, E.; Gilardi, R. *Chem. Commun.* **1999**, 173. (b) Guo, W. Z.; Galoppini, E.; Gilardi, R.; Rydja, G. I.; Chen, Y. H. *Cryst. Growth Des.* **2001**, *1*, 231.
- <sup>5</sup>(a) Kitazawa, T.; Nishikiori, S.; Kuroda, R.; Iwamoto, T. *Chem. Lett.* **1988**, 1729. (b) Kitazawa, T.; Nishikiori, S.; Yamagishi, A.; Kuroda, R.; Iwamoto, T. *Chem. Commun.* **1992**, 413.
- <sup>6</sup>(a) Copp, S. B.; Subramanian, S.; Zaworotko, M. J. *J. Am. Chem. Soc.* **1992**, *114*, 8719. (b) Zaworotko, M. J. *Chem. Soc. Rev.* **1994**, 283. (c) Copp, S. B.; Holman, K. T.; Sangster, J. O. S.; Subramanian, S.; Zaworotko, M. J. *J. Chem. Soc., Dalton Trans.* **1995**, 2233.
- <sup>7</sup>(a) Carlucci, L.; Ciani, G.; Proserpio, D. M.; Sironi, A. *Chem. Commun.* **1994**, 2755. (b) Carlucci, L.; Ciani, G.; Proserpio, D. M.; Rizzato, S. *Chem.-Eur. J.* **2002**, 1520.
- <sup>8</sup>Reddy, D. S.; Dewa, T.; Endo, K.; Aoyama, Y. *Angew. Chem., Int. Ed.* **2000**, *39*, 4266.
- <sup>9</sup>(a) Evans, O. R.; Xiong, R.-G.; Wang, Z.; Wong, G. K.; Lin, W. *Angew. Chem., Int. Ed.* **1999**, *38*, 526. (b) Evans, O. R.; Wang, Z.; Xiong, R.-G.; Foxman, B. M.; Lin, W. *Inorg. Chem.* **1999**, *38*, 2969. (c) Lin, W.; Ma, L.; Evans, O. R. *Chem. Commun.* **2000**, 2263. (d) Evans, O. R.; Lin, W. *Acc. Chem. Res.* **2002**, *35*, 511.
- <sup>10</sup>Thaimattam, R.; Sharma, C. V. K.; Clearfield, A.; Desiraju, G. R. *Cryst. Growth Des.* **2001**, *1*, 103.
- <sup>11</sup>(a) Hoskins, B. F.; Robson, R. *J. Am. Chem. Soc.* **1989**, *111*, 5962. (b) Hoskins, B. F.; Robson, R. *J. Am. Chem. Soc.* **1990**, *112*, 1546.
- <sup>12</sup>A variety of binary inorganic compounds with nonlinear optical properties are known to belong to this class. See: (a) Flytzanis, C. Nonlinear Polarization. In *Nonlinear Optical Materials: Principles and Applications*; Degiorgio, V., Flytzanis, C., Eds.; IOS Press: Washington, 1995; pp 3 and 97. (b) Tang, C. L. Optical Parametric Processes and Inorganic Nonlinear Optical Crystals. In *Nonlinear Optical Materials: Principles and Applications*; Degiorgio, V., Flytzanis, C., Eds.; IOS Press: Washington, 1995; pp 3 and 97.
- <sup>13</sup>To the best of our knowledge, only Reddy and Desiraju proceeded with attempts of molecular assembly of this type. See: (a) Reddy, D. S.; Craig, D. C.; Rae, A. D.; Desiraju, G. R. *Chem. Commun.* **1993**, 1737. (b) Reddy, D. S.; Craig, D. C.; Desiraju, G. R. *Chem. Commun.* **1994**, 1457.
- <sup>14</sup>The Braggs concluded their historic communication entitled “*The Structure of the Diamond*” with the succinct statement: “...Zinblendes appears to have the same structure, but the (111) planes contain alternately only zinc and only sulfur atoms. In this way the crystal acquires polarity and becomes hemihedral...” See: Bragg, W. H.; Bragg, W. L. *Nature* **1913**, *91*, 557.
- <sup>15</sup>We note that tetrahedral blocks can be assembled in a variety of ways including diamondoid as well as hexagonal networks. For example, the diamondoid cubic structure of ice (*lc*) is metastable and irreversibly transforms into regular hexagonal ice (*lh*), the marginal enthalpy difference being less than 0.05 kJ mol<sup>-1</sup>. [See: Petrenko, V. F.; Whitworth, R. W. *Physics of Ice*; Oxford University Press: New York, 1999; pp 276–277.] The diamondoid/hexagonal relationship for the assembly of tetrahedral elements is dependent on close molecular packing, for example, as recently shown by the nature of encapsulated guest molecules in clathrate complexes by: Kitazawa, T.; Kikuyama, T.; Takeda, M.; Iwamoto, T. *J. Chem. Soc., Dalton Trans.* **1995**, 3715.
- <sup>16</sup>This problem was identified from the very first attempts at diamondoid designs. For example, the single diamondoid network built from adamantanetetracarboxylic acid<sup>3</sup> should have a calculated density of 0.336 g/cm<sup>3</sup>, that is, merely 20% of that expected (about 1.5 g/cm<sup>3</sup>) for organic compounds. Nevertheless, a possibility of the stabilization and utilization of such “organic zeolites” appears to be very attractive. See, for example: Aoyama, Y. *Top. Curr. Chem.* **1998**, *198*, 132.
- <sup>17</sup>Batten, S. R.; Robson, R. *Angew. Chem., Int. Ed.* **1998**, *37*, 1460.
- <sup>18</sup>Hirsch, K. A.; Wilson, S. R.; Moore, J. S. *Chem.-Eur. J.* **1997**, *3*, 765.
- <sup>19</sup>Thus, Kitazawa, Iwamoto, et al.<sup>5</sup> have shown that, in the presence of CCl<sub>4</sub> or CMe<sub>4</sub>, Cd(CN)<sub>2</sub> forms only a single diamondoid motif with the cavities filled out by the tetrahedral guest solvent molecules. [In the absence of

the suitable guest molecules,  $\text{Cd}(\text{CN})_2$  itself produces crystals stabilized by the interpenetration of two identical diamondoid motifs.] In his pioneering work,<sup>11</sup> Robson also obtained extra-large diamondoid cells because of the clathration of a large excess (up to 8 molar equiv) of nitrobenzene solvent into the otherwise almost empty cages (containing just a single  $\text{BF}_4$  counterion). However, this approach did not become popular (except for works of Wuest<sup>2</sup> and Desiraju<sup>13b</sup>) – mainly because of the significant volatility of the exceedingly solvated clathrate crystals.<sup>20</sup>

- <sup>20</sup>It should be mentioned that the close-packing principle sometimes can be satisfied by the combination of interpenetration and clathration within the same crystal. See, for example: Zhang, J.; Lin, W.; Chen, Z.-F.; Xiong, R.-G.; Abrahams, B. F.; Fun, H.-K. *J. Chem. Soc., Dalton Trans.* **2001**, 1806.
- <sup>21</sup>This solution of the close-packing issue for large diamondoid networks was early demonstrated by Robson<sup>11b</sup> who showed that the presence of  $\text{NMe}_4^+$  counterion only in one-half of the cavities of the solitary<sup>22</sup>  $\text{Cu}^{\text{I}}\text{Zn}^{\text{II}}(\text{CN})_4$  diamondoid network was sufficient to complete (structural) stabilization. Yet thereafter this approach did not become popular.<sup>23</sup>
- <sup>22</sup>The pristine structure of the diamondoid network from  $[\text{Zn}(\text{CN})_2]$  is two-fold interpenetrated.<sup>11b</sup>
- <sup>23</sup>The void space in the large diamondoid networks can be compensated by the combination of counterion filling and solvent clathration<sup>11</sup> (cf. ref 20).
- <sup>24</sup>(a) Kapustinskii, A. F.; Drakin, S. I. *Izv. Akad. Nauk SSSR, Otdel. Chim. Nauk* **1950**, 233. (b) Strieter, F. J.; Templeton, D. H. *J. Chem. Phys.* **1962**, 37, 161.
- <sup>25</sup>(a) Cheeseman, G. H.; Whitaker, A. M. B. *Proc. R. Soc. London, Ser. A* **1952**, 212, 406. (b) Rastogi, R. P.; Nigam, R. K. *Trans. Faraday Soc.* **1955**, 51, 323. (c) Stavely, L. A. K.; Topman, W. I.; Hart, K. R. *Trans. Faraday Soc.* **1955**, 51, 323. (d) Noordtzi, R. M. A. *Helv. Chim. Acta* **1956**, 39, 637. (e) Goates, J. R.; Sullivan, R. J.; Ott, J. B. *J. Phys. Chem.* **1959**, 63, 589. (f) Stevenson, D. P.; Coppinger, G. M. *J. Am. Chem. Soc.* **1962**, 84, 149. (g) Anderson, R.; Prausnitz, J. M. *J. Chem. Phys.* **1963**, 39, 1225; **1964**, 40, 3443. (h) Weimer, R. F.; Prausnitz, J. M. *J. Chem. Phys.* **1965**, 42, 3643. (i) Chantry, G. W.; Gebbie, H. A.; Mirza, H. N. *Spectrochim. Acta* **1967**, 23A, 2749. (j) Davis, K. M. C.; Farmer, M. F. *J. Chem. Soc. B* **1967**, 28. (k) Rosseinsky, D. R.; Kellawi, H. *J. Chem. Soc. A* **1969**, 1207. (l) Tamres, M.; Strong, R. L. *Mol. Assoc.* **1979**, 2, 332.
- <sup>26</sup>(a) Blackstock, S. C.; Lorand, J. P.; Kochi, J. K. *J. Org. Chem.* **1987**, 52, 1451. (b) Blackstock, S. C.; Kochi, J. K. *J. Am. Chem. Soc.* **1987**, 109, 2484.
- <sup>27</sup>For molecular crystals, the large magnitude of nonlinear optical properties is expected from intramolecular electronic coupling between donor and acceptor groups. See: (a) Kanis, D. R.; Ratner, M. A.; Marks, T. *J. Chem. Rev.* **1994**, 94, 195. (b) Meyers, F.; Marder, S. R.; Pierce, B. M. N.; Bredas, J. L. *J. Am. Chem. Soc.* **1994**, 116, 10703. (c) *Nonlinear Optics of Organic Molecules and Polymers*; Naiva, H. S., Miyata, S., Eds.; CRC Press: New York, 1997. However, the intermolecular electronic coupling between donor and acceptor species may have the same effect.
- <sup>28</sup>(a) Creighton, J. A.; Thomas, K. M. *J. Mol. Struct.* **1971**, 7, 173. (b) Creighton, J. A.; Thomas, K. M. *J. Chem. Soc., Dalton Trans.* **1972**, 403. (c) Creighton, J. A.; Thomas, K. M. *J. Chem. Soc., Dalton Trans.* **1972**, 2254.
- <sup>29</sup>Lindner, H. J.; Kirschke-von Gross, B. *Chem. Ber.* **1976**, 109, 314.
- <sup>30</sup>In ref 13a, the  $(\text{Br}_3\text{CBr}\cdots\text{NR}_3)$  interactions are described as “weak” despite the observed interatomic separation of only 2.6 Å (which is 0.8 Å shorter than the corresponding equilibrium van der Waals separation<sup>31</sup>) and with previous measurements of reasonable values of the complex formation constant of 3.2  $\text{M}^{-1}$  in solutions.<sup>26a</sup>
- <sup>31</sup>Bondi, A. *J. Phys. Chem.* **1964**, 68, 441.
- <sup>32</sup>The formation constants of the  $[\text{CBr}_4\cdots\text{Cl}^-]$  complex are 2.03 and 4.78  $\text{M}^{-1}$  in dichloromethane and acetonitrile solutions, respectively, as determined earlier from vibrational spectra.<sup>28a,c</sup> Also, from the solid-state vibration spectra and some preliminary X-ray powder diffraction data, the lattice force constants of the various  $(\text{CBr}_4\cdots\text{halide})$  interactions were found to be in the range of 0.1–0.2  $\text{mdyn}/\text{Å}$ .<sup>28a,b</sup>

- <sup>33</sup>Drago, R. S. *Physical Methods in Chemistry*; Saunders: Philadelphia, 1977.
- <sup>34</sup>This is in agreement with the earlier data based on the measurement of the electrical conductivity of solutions.<sup>28c</sup>
- <sup>35</sup>For the  $[\text{CBr}_4, \text{Cl}^-]$  complex, the new band appears as a shoulder of the  $\text{CBr}_4$  absorption. Therefore, differential spectra were calculated, and Gaussian simulation was applied to properly evaluate its parameters.
- <sup>36</sup>The  $[\text{CBr}_4, \text{I}^-]$  complex is light sensitive in solution and should be kept in the dark. Under the light radiation, the new absorbance arises pertinent to  $\text{I}_3^-$  ion formation. However, no further study on the photochemistry of this system was attempted as yet. The salt  $(\text{NPr}_4^+\text{I}^-)$  absorbs at  $\lambda_{\text{max}} = 245 \text{ nm}$  ( $\epsilon_{245} = 1.7 \times 10^4 \text{ M}^{-1} \text{ cm}^{-1}$ ).
- <sup>37</sup>(a) Mulliken, R. S. *J. Am. Chem. Soc.* **1952**, *74*, 811. (b) Mulliken, R. S.; Person, W. B. *Molecular Complexes*; Wiley: New York, 1969.
- <sup>38</sup>Benesi, H. A.; Hildebrand, J. H. *J. Am. Chem. Soc.* **1949**, *71*, 2703.
- <sup>39</sup>Typical values of the formation constant  $K_{\text{EDA}}$  for organic charge-transfer complexes lie in the 0.1–10  $\text{M}^{-1}$  range. See: (a) Andrews, L. J.; Keefer, R. M. *Molecular Complexes in Organic Chemistry*; Holden-Day: San Francisco, CA, 1964. (b) Foster, R. *Organic Charge-Transfer Complexes*; Academic: New York, 1973. (c) Briegleb, G. *Electronen-Donator-Acceptor Komplexe*; Springer: Berlin, 1961.
- <sup>40</sup>(a) Hush, N. S. *Prog. Inorg. Chem.* **1967**, *8*, 391. (b) Hush, N. S. *Electrochim. Acta.* **1968**, *13*, 1005.
- <sup>41</sup>The typical values of the electronic coupling element in organic charge-transfer complexes are 0.1–0.6 eV. For example, the CT complexes of chloranil with aromatic (alkylbenzene) donors have  $H_{\text{AB}}$  in the range of 0.2–0.5 eV. See: Rosokha, S. V.; Kochi, J. K. In *Modern Arene Chemistry*; Astruc, D., Ed.; VCH-Wiley: New York, 2002; pp 435ff.
- <sup>42</sup>Hoskins and Robson<sup>11b</sup> (who already addressed this question for the positioning of  $\text{NMe}_4^+$  ions in the  $\text{Zn}_4\text{Cu}_6$  cavities of the  $[\text{CuZn}(\text{CN})_4]^-$  anionic network) assumed that these two types of cavities possess a different “amount of electric charge”. From the point of view of crystal symmetry, this assumption is probably incorrect; yet these two types of cavities do possess quite different (either tetrahedral or octahedral) symmetry of electrostatic potential. In our case, the tetrahedral ammonium ion occupies cavities with symmetrically aligned (tetrahedral) arrangements of halide.
- <sup>43</sup>This crystal arrangement was predicted earlier for the  $[\text{Et}_4\text{N}^+\text{Cl}^-, \text{CBr}_4]$  complex from unpublished powder diffraction data (see ref 28a); the symmetry of the corresponding isostructural  $[\text{Et}_4\text{N}^+\text{Br}^-, \text{CBr}_4]$  and  $[\text{Et}_4\text{N}^+\text{I}^-, \text{CBr}_4]$  complexes at that time was mistakenly attributed to cubic syngony.
- <sup>44</sup>We found the crystals of  $[\text{Et}_4\text{N}^+\text{Br}^-, \text{CBr}_4]$  to exhibit a phase transition into the cubic symmetry above 25 °C. However, the complete structural study was discouraged by the experimental difficulties of consistently maintaining an elevated temperature over prolonged times.
- <sup>45</sup>The anisometric swastika-like shape of the cations is somewhat elongated in the direction of the inversion four-fold axis ( $S_4$ -symmetry) that results in the increase of the  $c$ -parameter of the I-centered tetragonal cell by 7.6%, 8.4%, and 10.2% (from halide = Cl to I, respectively) relative to the ideal values required by the F-centered cubic cell. For an example of the similar effect of guest molecules on the symmetry of diamondoid networks, see: Kitazawa, T. *Chem. Commun.* **1999**, 891.
- <sup>46</sup>In an only early known ( $\text{CBr}_4/\text{halide}$ ) crystal structure  $[\text{Ph}_4\text{P}^+\text{Br}^-, \text{CBr}_4]$ ,<sup>29</sup> the charge-transfer motif is built up of one-dimensional centrosymmetric bands  $[\text{Br} \cdots \text{CBr}_4]_n$  because of the large size of the bulky  $\text{Ph}_4\text{P}^+$  counterions that dominate the structure.
- <sup>47</sup>DBU- $\text{H}^+\text{Br}^-$  is 1-aza-8-azoniabicyclo(5.4.0)undec-7-ene bromide and contains a single  $(\text{CN}^+\text{HC})$  cationic center.
- <sup>48</sup>Additional  $\text{CBr}_4$  acceptors enter into the  $(\text{halide})_4(\text{CBr}_4)_6$  cages of the original diamondoid network, and this results in a combination of two equivalent intersecting diamondoid networks having common (Br $^-$ ) nodes. Effectively, the bridging (Br $^-$ ) donors become not four, but eight-coordinated. This higher coordination number is very unusual for (Br $^-$ ) ions and yields substantially longer (CBr $\cdots$ Br $^-$ ) charge-transfer separations of 3.332 Å, which are still 0.37 Å shorter than the corresponding van der Waals separation.<sup>31</sup> The  $\text{Me}_4\text{N}^+$  counterions are

disordered in the rhombocubooctahedral cavities of this centrosymmetric network to comply with the dissimilar symmetry of the voids.

- <sup>49</sup>Because the earlier data<sup>50</sup> on the geometry of pristine CBr<sub>4</sub> were of low precision, we redetermined its structure at -150 °C. In the four symmetrically independent molecular units, the C–Br bond lengths vary within the range 1.920–1.940(5) Å with av. 1.930 Å. In the structures of the tetraethylammonium complexes [Et<sub>4</sub>N<sup>+</sup>halide<sup>-</sup>, CBr<sub>4</sub>], these bonds are 1.953–1.957(2) Å.
- <sup>50</sup>More, M.; Baert, F.; LeFebvre, J. L. *Acta Crystallogr., Sect. B* **1977**, *33*, 3681.
- <sup>51</sup>As an example, Evans, Lin, and co-workers deliberately utilized the absence of inversion symmetry in the odd-order (interpenetrated) diamondoid networks to assemble a variety of interesting noncentrosymmetric crystal structures exhibiting SHG activity.<sup>9d</sup>
- <sup>52</sup>For example, strong electron  $\sigma$ -coupling is the source of the unsurpassed hardness of diamond itself<sup>53</sup> as well as the partial electron delocalization responsible for the unique semiconductive properties of silicon and germanium (diamondoid) crystals. Without such interactions, the diamondoid three-dimensional ordering does not have any specific advantage other than an aesthetics. Some recent papers already address this problem, referring to electronic spin interactions between diamondoid nodes to produce materials with advanced magnetic properties.<sup>54</sup>
- <sup>53</sup>Some interesting views on the electronic origins of the hardness of the diamond and diamondlike materials can be found in: Proserpio, D. M.; Hoffmann, R.; Preuss, P. *J. Am. Chem. Soc.* **1994**, *116*, 9634.
- <sup>54</sup>(a) Mathevet, F.; Luneau, D. *J. Am. Chem. Soc.* **2001**, *123*, 7465. (b) Gieck, C.; Rocker, F.; Ksenofontov, V.; Gütlich, P.; Tremel, W. *Angew. Chem., Int. Ed.* **2001**, *40*, 908.
- <sup>55</sup>For binary (covalent) diamondoid crystals such as GaAs or InP, the large hyperpolarizability values were shown to arise from the charge asymmetry along the heteropolar bonds.<sup>12a</sup>
- <sup>56</sup>The crystalline powders of the charge-transfer complex [Et<sub>4</sub>N<sup>+</sup>Br<sup>-</sup>, CBr<sub>4</sub>] show relatively strong SHG-intensity that appeared to be phase-matchable, and 500 times larger than the SHG response of quartz. Two other samples show similar SHG behavior.
- <sup>57</sup>Perrin, D. D.; Armarego, W. L. F.; Perrin, D. R. *Purification of Laboratory Chemicals*; Pergamon Press: New York, 1980.
- <sup>58</sup>Similar (irreversible) oxidation anodic peaks for halide ions were obtained previously in acetonitrile (but systematically shifted by ca. +0.25 V relative to those measured in dichloromethane). See: Ebersson, L. *Electron-Transfer Reactions in Organic Chemistry*; Springer-Verlag: New York, 1987. These values are related to the gas-phase electron affinities of the halogen atoms of 3.61 (Cl<sup>•</sup>), 3.36 (Br<sup>•</sup>), and 3.06 (I<sup>•</sup>) eV, see: Dean, J. A. *Lange's Handbook of Chemistry*, 15th ed.; McGraw-Hill: New York, 1999.
- <sup>59</sup>Howell, J. O.; Goncalves, J. M.; Amatore, C.; Klasinc, L.; Wightman, R. M.; Kochi, J. K. *J. Am. Chem. Soc.* **1984**, *106*, 3968.
- <sup>60</sup>Sheldrick, G. M. *SADABS (Ver. 2.03) – Bruker/Siemens Area Detector Absorption and Other Corrections*; 2000.
- <sup>61</sup>Sheldrick, G. M. *SHELXS 86 – Program for Crystal Structure Solutions*; University of Göttingen: Germany, 1986.
- <sup>62</sup>Sheldrick, G. M. *SHELXL 93 – Program for Crystal Structure Refinement*; University of Göttingen: Germany, 1993.
- <sup>63</sup>Kurtz, S. K.; Perry, T. T. *J. Appl. Phys.* **1968**, *39*, 3798.
- <sup>64</sup>The powder X-ray diffraction pattern of the sample supplied for the measurements of the second harmonics generation coincided with the powder diffraction pattern simulated from the single-crystal X-ray measurements as described in Figure S4 in the Supporting Information. This result confirms the crystallographic authenticity of the samples used for the structural/optical measurements.